ECI Symposium Series, Volume RP2: Proceedings of 6th International Conference on Heat Exchanger Fouling and Cleaning - Challenges and Opportunities, Editors Hans Müller-Steinhagen, M. Reza Malayeri, and A. Paul Watkinson, Engineering Conferences International, Kloster Irsee, Germany, June 5 - 10, 2005

Measurement of Particle-Fluid Velocities of a Particle Containing Fluid Flow in a Grooved Channel

Dong-Xu Jin[1], Dae-Young Lee[2] and Yoon-Pyo Lee[3]

[1] Thermal/Flow Control Research Center, Korea Institute of Science and Technology, Seoul 136-791, Korea, dxjin@postech.ac.kr
[2] Thermal/Flow Control Research Center, Korea Institute of Science and Technology, Seoul 136-791, Korea, ldy@kist.re.kr
[3] Thermal/Flow Control Research Center, Korea Institute of Science and Technology, Seoul 136-791, Korea, yplee@kist.re.kr

ABSTRACT

A novel method for simultaneously measuring the fluid velocity and the large particle velocity in a particle-containing fluid flow is developed in this study. In this method, the velocities of the fluid and the large particle are measured by PIV and PTV, respectively, from the same flow images taken by a single CCD camera. Since a PIV result represents the average displacement of all the particles in an interrogation window, it will include an error caused by the relative displacement of the large particles as compared with the fluid. In order to reduce the false influence from large particles on the PIV calculation, the mean brightness of small PIV particle images is substituted for the locations of large particles in the PIV images. The simulation results showed that the new method can significantly reduce the PIV error caused by the large particles. The newly developed method is also applied to an actual case of the particle-containing fluid flow in a triangular grooved channel. In this case, the large particles flowing into the groove slow down gradually and eventually deposit on the groove surface, while the fluid in the groove rotates to form a steady vortex. Regardless of the velocity difference between the particles and the fluid, the fluid velocity can be measured correctly employing the novel method. The new method can be applied to the investigation of particulate fouling problems.

INTRODUCTION

The relative flow behavior of the particle to the fluid is a key factor for the investigation of the processes pertinent to the particle-containing fluid flows, such as filtration and particulate fouling. If the particle size is large or the density is not very close to the fluid, the velocity of the particle tends to deviate from that of the fluid owing to the effects of buoyancy and inertia. In such cases, it is important to investigate the mutual interaction between the fluid and the particle. To this end, the information is required on the individual velocities of both the particle and the fluid at an instant. Consequently, the particle velocity and the fluid velocity should be measured simultaneously.

In many cases, the fluid velocity can be measured using a PIV method and the particle velocity using a PTV method. In a particle-containing fluid flow, the PIV tracer particles added to the fluid for the PIV investigation should be small enough to be distinguishable from the particles inherently contained in the fluid. It is recommended that the diameter of the tracer particles be about 0.1 times smaller compared with the inherently contained particles (Wereley et al., 2002). In this respect, hereafter we call the particles inherently contained in the fluid as the large particles and the PIV tracer particles as the small particles.

Choi et al. (2002) investigated the motion of a particle/bubble in a vertical pipe using two CCD cameras. The fluid velocity and the particle velocity were measured using PIV and PTV, respectively. In order to avoid the interference between the PIV and PTV, optical filters with different ranges of wavelength were used for both the stroboscope and CCD cameras. Also, the fluorescent tracer particles were used in PIV measurement.

Wereley et al. (2002) measured both the particle velocity and the fluid velocity in a rotating filter at a cross-section perpendicular to the rotation shaft using PIV and PTV. The images for both PIV and PTV analyses were obtained simultaneously using a single CCD camera. The images for PTV analysis were obtained by extracting only the large particles from the native images taken by the CCD camera based on their brightness and sizes. Then, the images with the large particles being removed to leave only PIV tracer particles were used for the PIV analysis. In their measurement, the volume concentration of the large particles was limited very small, i.e., around 10^{-4} (m^3 particle/m^3 fluid) which corresponds to an area fraction of only about 0.1-0.5% in the PIV image.

Since the PIV result statistically represents the average displacement of all the particles in PIV images, it is inevitable that the result includes the influence of the large particles' displacement if the large particles appear in the images. Therefore, if the large particles' velocity differs from the fluid velocity, the PIV result can not represent correctly the fluid displacement when using a single camera to obtain the images for both the PIV and the PTV simultaneously. Consequently, in order to evaluate accurately the fluid velocity in a particle-containing fluid flow, the influence of large particles should be excluded before the PIV analysis.

In this study, we developed a new method to minimize the false influence of large particles in the PIV analysis. With this method, it is possible to proceed with both the PIV and the PTV analyses to get the simultaneous velocities of the fluid and the large particles using the same set of images containing all the small and large particles. This method can be applied even to a flow where the concentration of large particle is so high that the area fraction of the large particles in the image reaches several tens of percents. For the verification of this new method, a case of particulate deposit in a triangular grooved channel is analyzed employing this method to investigate the flow characteristics of the fluid and the large particles.

SIMULTANEOUS MEASUREMENT TECHNIQUE

Single exposure/double frame, cross-correlation based PIV is probably the most commonly used method in PIV. This method uses two serial images of tracer particles to calculate relative displacement of the particles, as shown schematically in Figs. 1 and 2. The displacement is evaluated for each sub-image (interrogation window) taken from the PIV image by subdividing it into multiple small images. The interrogation window A_g in the second image is taken larger than the interrogation window A_f in the first image such that it may include all the possible displacements of the particles within A_f. The average spatial displacement of particles can be estimated through a statistical technique of cross-correlation between the interrogation windows A_f and A_g. The cross-correlation is given by

$$R(\mathbf{s}) = \int_{A_f} f(\mathbf{x}) g(\mathbf{x}+\mathbf{s}) d\mathbf{x} \qquad (1)$$

where f and g are the respective brightness functions of A_f and A_g, and $\mathbf{s}$ is the separation vector between A_f and A_g as shown in Fig. 2. From a statistical point of view, the separation vector showing the highest correlation peak represents the relative displacement for the best match between the interrogation windows A_f and A_g (Gonzalez and Woods, 2002).

If large particles with different velocities than the small PIV particles are included in the interrogation windows, the correlation function will be affected by the large particles. As a result, the displacement of small PIV particles determined based on the correlation function is distorted by the large particles. Fig. 2 is a schematic presentation to show the influence of the large particle on the cross-correlation. It can be seen that there exist two local correlation peaks corresponding to the best matches for the small PIV particles and for the large particle, respectively. Even if the image of large particle is removed from both the interrogation windows by substituting zero brightness to the area occupied by the large particle, the influence of large particle will not vanish because the correlation still exists between the areas having zero brightness. In order to reduce the influence of large particles on the PIV result, it is required to replace the large particles in the native images with a constant non-zero brightness to minimize distortion of the correlation function caused by the existence of the large particles.

On the other hand, the velocity of each large particle can be obtained from the match probability based two-frame PTV analysis (Ohmi and Li, 2000). The images of the large particles for the PTV analysis can be extracted from the native images if the large particles can be easily identified

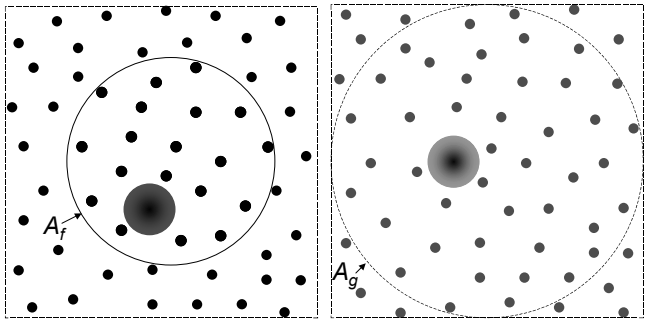

(a) interrogation window A_f (b) interrogation window A_g

Fig. 1. Schematics of serial images for PIV analysis of a particle-containing fluid flow.

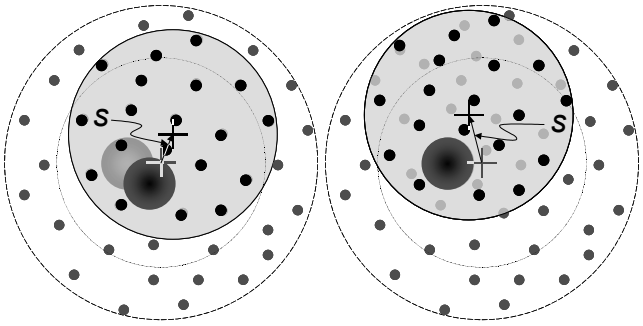

(a) best match for the fluid (b) best match for a large particle

Fig. 2. Correlating process between interrogation areas f and g in the PIV calculation.

based on the brightness and size of the particles. In this case, the PTV result is hardly affected by the existence of small PIV particles.

Derivation of optimal replacement brightness value for the large particles

Let's consider first the case where in the two serial CCD images, only one CCD image has large particles while no large particles exist in the other CCD image. In this case, if we take the interrogation window A_f from the large particle existing image, the cross-correlation can be expressed as

$$R_f(\mathbf{s}) = \int_{A_f - \sum_{i=1}^{n} A_{p,i}} f(\mathbf{x}) g(\mathbf{x}+\mathbf{s}) d\mathbf{x} + \alpha \int_{\sum_{i=1}^{n} A_{p,i}} g(\mathbf{x}+\mathbf{s}) d\mathbf{x} \tag{2}$$

where n and $A_{p,i}$ are the number of the large particles and the area occupied by the i^{th} large particle, respectively, and α is the brightness value to replace the large particles. The difference in the correlation between the cases with and without large particles can be given by subtracting Eq. (1) from Eq. (2) as

$$\begin{aligned} \Delta R_f = R_f - R &= \int_{\sum_{i=1}^{n} A_{p,i}} [\alpha - f(\mathbf{x})] g(\mathbf{x}+\mathbf{s}) d\mathbf{x} \\ &\approx \sum_{i=1}^{n} A_{p,i} [\alpha - f(\mathbf{X}_i)] g(\mathbf{X}_i + \mathbf{s}) \end{aligned} \tag{3}$$

where $\mathbf{X}_i$ is the position vector to the center of the i^{th} large particle. In the simplification of the above equation, the areas occupied by the large particles are presumed extremely small compared with the interrogation area, A_f.

Equation (3) implies the distortion of the correlation function due to the existence of the large particles. In order to minimize the correlation difference for any positions of the large particles and any fluid displacement, the replacement brightness should satisfy the following equation

$$\frac{d}{d\alpha} \int_{A_f} d\mathbf{X}_1 \cdots \int_{A_f} d\mathbf{X}_n \int_{A_s} \Delta R_f^2 d\mathbf{s} = 0 \tag{4}$$

where A_s is the domain of the separation vector, which includes the largest possible relative displacement between A_f and A_g.

Substituting Eq. (3) into the left hand side of Eq. (4) yields

$$\begin{aligned} &\frac{d}{d\alpha} \int_{A_f} d\mathbf{X}_1 \cdots \int_{A_f} d\mathbf{X}_n \int_{A_s} \Delta R_f^2 d\mathbf{s} \\ &\quad = 2 \int_{A_f} \sum_{i=1}^{n} A_{p,i} [\alpha - f(\mathbf{X}_i)] G_i d\mathbf{X}_i \end{aligned} \tag{5}$$

where G_i is the abbreviated expression of the following:

$$\begin{aligned} G_i = &\int_{A_f} d\mathbf{X}_1 \cdots \int_{A_f} d\mathbf{X}_{i-1} \int_{A_f} d\mathbf{X}_{i+1} \\ &\cdots \int_{A_f} d\mathbf{X}_n \int_{A_s} \sum_{j=1}^{n} A_{p,j} g(\mathbf{X}_i + \mathbf{s}) g(\mathbf{X}_j + \mathbf{s}) d\mathbf{s} \\ = &A_f^{n-2} \sum_{\substack{j=1 \\ j \neq i}}^{n} A_{p,j} \int_{A_f} d\mathbf{X}_j \int_{A_s} g(\mathbf{X}_i + \mathbf{s}) g(\mathbf{X}_j + \mathbf{s}) d\mathbf{s} \\ &+ A_f^{n-1} A_{p,i} \int_{A_s} g^2(\mathbf{X}_i + \mathbf{s}) d\mathbf{s} \end{aligned} \tag{6}$$

In the PIV analysis, the tracer particles should appear evenly distributed over the image, otherwise the location of the correlation peak is not only dependent on the velocity field, but is also biased depending on the distribution of the tracer particles (Westerweel, 1997). Therefore, in general, the brightness is distributed homogeneously in PIV images. In such cases, the following relation is satisfied regardless of the location of the large particle, **X**.

$$\frac{1}{A_s} \int_{A_s} g^2(\mathbf{X}+\mathbf{s}) d\mathbf{s} \approx const \equiv \langle g^2 \rangle \tag{7}$$

$$\frac{1}{A_s} \int_{A_s} g(\mathbf{X}+\mathbf{s}) d\mathbf{s} \approx const \equiv \langle g \rangle \tag{8}$$

Substitute Eqs. (7) and (8) into Eq.(6) to get

$$\begin{aligned} G_i &\approx A_f^{n-1} \langle g \rangle \sum_{\substack{j=1 \\ j \neq i}}^{n} A_{p,j} \int_{A_s} g(\mathbf{X}_i + \mathbf{s}) d\mathbf{s} + A_f^{n-1} A_{p,i} A_s \langle g^2 \rangle \\ &\approx A_f^{n-1} A_s \left(\langle g \rangle^2 \sum_{\substack{j=1 \\ j \neq i}}^{n} A_{p,j} + A_{p,i} \langle g^2 \rangle \right) = const > 0 \end{aligned} \tag{9}$$

Substituting Eq. (9) into Eq. (5), and then the result into the left hand side of Eq. (4) yields

$$\left(\sum_{i=1}^{n} A_{p,i} G_i\right) \int_{A_f} [\alpha - f(\mathbf{X}_i)] d\mathbf{X}_i = 0 \qquad (10)$$

To satisfy Eq. (10), the optimum brightness, α, to replace the particles is given by

$$\alpha = \frac{1}{A_f} \int_{A_f} f(\mathbf{X}) d\mathbf{X} = \langle f \rangle \qquad (11)$$

This result implies that when only one CCD image has large particles while there is no large particle in the other CCD image, the optimum brightness to replace the large particles in each interrogation window is the mean brightness of the small PIV particles in the same interrogation window.

Now, let's consider the case where large particles exist in both serial CCD images. If we neglecting the effect of the large particles in the interrogation window A_f overlapping with those in the interrogation window A_g, the correlation difference is given by:

$$\Delta R = \Delta R_f + \Delta R_g \qquad (12)$$

where ΔR_g is the correlation difference when the large particles exist only in the interrogation window A_g.

Since ΔR_f and ΔR_g are independent to each other, to minimize ΔR equals to minimize ΔR_f and ΔR_g separately. Therefore, even when both the CCD images have large particles, the optimum replacement value for the large particles is still the mean brightness of the small PIV particles.

As mentioned in the previous section, the displacement of the large particle affects the correlation function and thus the PIV result. To prevent this effect, it is required to make the large particle more difficult to find its corresponding pair from the correlating image. This can be accomplished by modifying the image of the large particle to make it more undistinguishable from the background image. From the statistical point of view, the best modification of the large particle is to replace the large particle with the mean brightness of interrogation window as arranged in this section.

Verification of the algorithm

The newly developed method was tested first with the artificially generated particle images. The images were generated by adding the images of large particles to the standard PIV images with a known velocity field (Okamoto et al., 2000). The interrogation window was set to be 32×32 pixels and 50% overlap was permitted. The randomly distributed large particles were square in shape with a uniform size of 7×7 pixels. The area occupied by the large particles is 20% of the interrogation window if not mentioned otherwise.

Figure 3(a) shows one of the artificial images used for the verification test. The large square white spots represent the large particles. The background images with the small particles were adopted from the work of Okamoto et al. (2000). The given fluid velocity field is shown in Fig. 3(b). The maximum fluid displacement was 6.2 pixels. The large particles were given a uniform displacement. The displacement of the large particles were obtained from PTV and shown in Fig. 3(c). The displacement was found consistent with the given value.

The effects of the replacement values for the images of large particles are shown in Fig. 3(e)-(h). When the images of large particles are replaced by the mean brightness of the interrogation window, the PIV analysis on the modified images obtains a result very close to the given velocity field as shown in Fig. 3(e) and (f).

Meanwhile, if the images of large particles are just removed and replaced by zero brightness, the PIV analysis results in a significant error as shown in Fig. 3(g) and (h). In this case, the error vectors shown in Fig. 4(h) can be classified into two groups: very large ones and extremely small ones. The very large error vectors are nearly the same as the velocity differences between the large particles and fluid shown in Fig. 3(d). This implies that the fluid displacement with the large PIV error is calculated as the displacement of the large particle instead of that of the fluid.

In order to investigate the reason for the two-state characteristics of the PIV error, the distribution of correlation function is shown schematically in Fig. 4 for the case of substituting zero brightness for the large particles. In this figure, s is the degree of the separation, l_p the size of the large particle, d_r the relative displacement of the large particle to the fluid, and R_0 is the background value when the interrogation windows A_f and A_g are completely not correlated. For the sake of simplicity, the displacement of fluid is assumed zero in this case such that there exists a local maximum of the correlation function at s=0.

Since the images of the large particles are substituted by zero brightness, the areas overlapped with the large particles are eliminated from the correlation calculation. The eliminated portion becomes the minimum when the large particles are completely overlapped with each other. Therefore, another local maximum in the correlation function exists at the separation corresponding to the displacement of the large particle.

As shown in Fig. 4, if the relative displacement between the large particle and the fluid is small, the highest

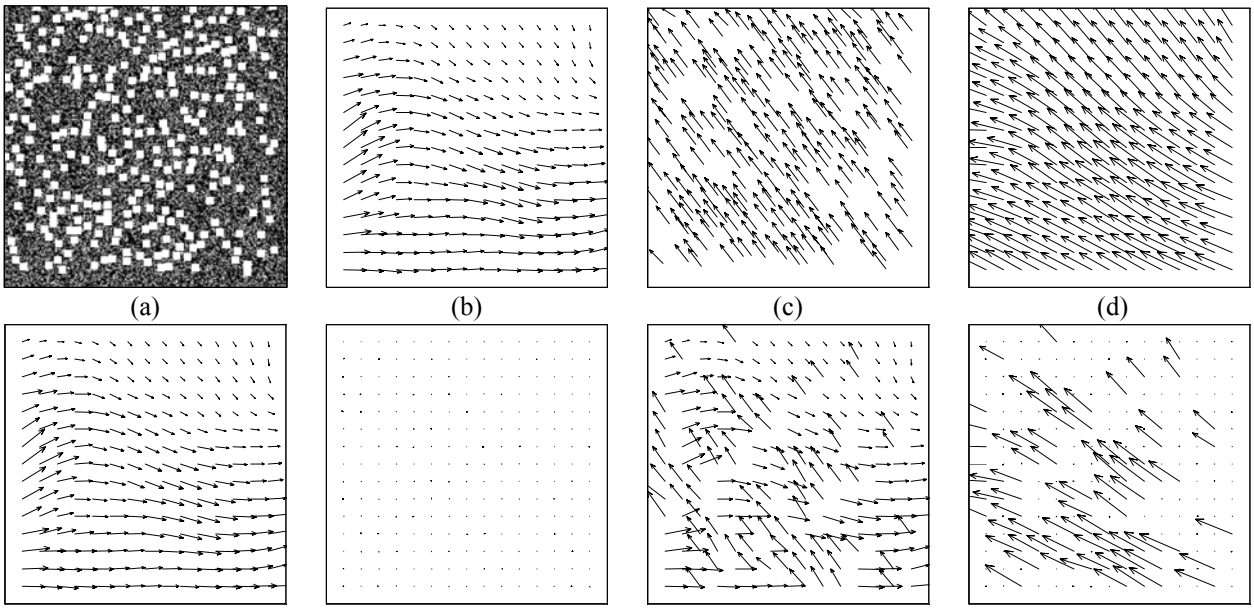

Fig. 3. Simulation results of PIV and PTV simultaneous measurement.
(a) PIV+PTV image, (b) given fluid velocity field, (c) PTV result, (d) velocity difference between the large particles and fluid; (e) PIV result: $\alpha = \langle f \rangle$, $\beta = \langle g \rangle$, (f) PIV error: $\alpha = \langle f \rangle$, $\beta = \langle g \rangle$, (g) PIV result: $\alpha = 0$, $\beta = 0$, (h) PIV error: $\alpha = 0$, $\beta = 0$

correlation peek occurs at the separation corresponding to the fluid displacement regardless of the relative displacement of the large particle. This is because the decrease in the local maximum value of the correlation corresponding to the fluid displacement is not very large since the most part of the large particles is overlapped with each other and the elimination is not very large. However, as the relative displacement between the large particle and the fluid increases, the correlation value corresponding to the fluid displacement becomes smaller and eventually smaller than the correlation value corresponding to the displacement of the large particle. At the instant, the separation for the highest correlation moves suddenly from the value corresponding to the displacement of the fluid to the value corresponding to the displacement of the large particle. This is the reason for the abrupt change and two-state characteristics of the PIV error shown in Fig. 3(g).

Figure 5 displays the effect of the brightness value to replace the large particle on the mean PIV error. The mean PIV error was defined as

$$E_{mean} = \frac{1}{N}\sum_{i=1}^{N}\left|\frac{d_i - d_{ai}}{l_p}\right| \qquad (13)$$

where N is the number of interrogation windows, and d_i and d_{ai} are the calculated and the exact displacements of i^{th} interrogation window. It is clear that substituting the mean brightness of small particles for the large particles effectively reduces the mean PIV error caused by the velocity difference between the large particles and fluid. The larger the brightness difference between the large particles and the small particles is, the larger is the mean

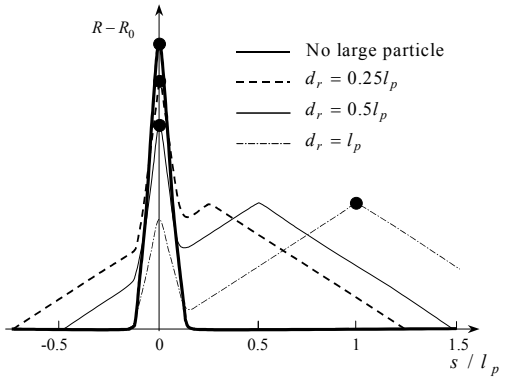

Fig. 4. Correlations for the different relative displacements between the large particles and fluid when $\alpha = 0$, $\beta = 0$.

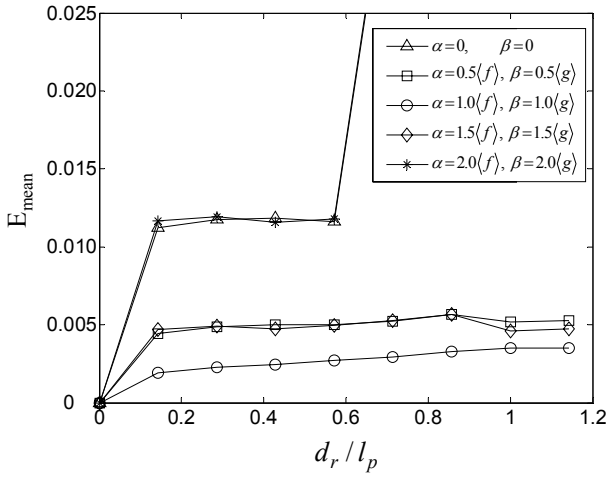

Fig. 5. Variation of the mean PIV error over the brightness of large particles.

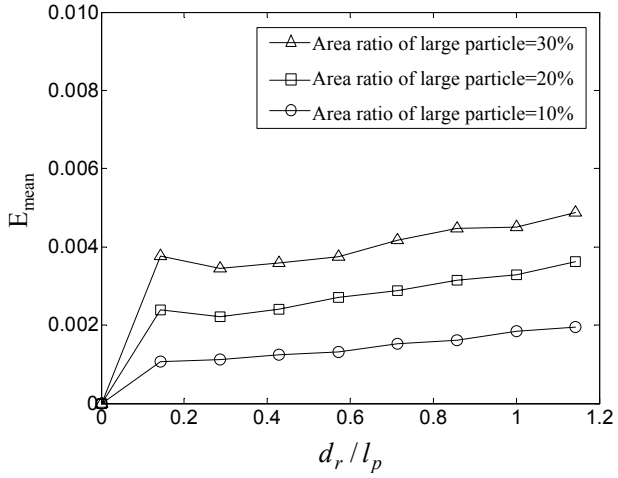

Fig. 6. Variation of the mean PIV error over the area fraction of large particles: $\alpha = \langle f \rangle$, $\beta = \langle g \rangle$.

PIV error. When the substituting brightness value for the large particles was twice as that of small particles, the mean PIV error varied gradually at first and then suddenly increased at some location around d_r/l_p =0.6. This means that the separation for the global maximum of the correlation changed from the fluid displacement to the displacement of large particles in some interrogation windows.

Figure 6 shows the effect of the relative size of the area occupied by the large particles in the whole image when the mean brightness of the small PIV particles was substituted for the locations of large particles. Though the mean PIV error is found to increase with an increase in the area fraction, the error is smaller than 0.5% even when the large particles occupy the area as large as 30% from the whole image.

APPLICATION OF THE METHOD TO A PARTICLE-CONTAINING FLUID FLOW IN A GROOVED CHANNEL

The simultaneous velocity measurement of the fluid and the particles has been carried out applying the newly developed method for a particle-containing fluid flow in a triangular grooved channel. Such kind of flow situation can be found in compact heat exchangers dealing with dirty fluids. In such cases, the information on the simultaneous velocities of the fluid and the particles is very important to investigate the interaction between the fluid and the particles and the particulate fouling characteristics.

The experimental setup is the same as that of Jin et al. (2004). Fig. 7 shows the triangular grooved channel having a height (*H*) of l5 mm, a length (*L*) of 18 mm and a depth (*a*) of 9 mm. The channel is composed of 30 grooves arranged in the flow direction and is 187.5 mm wide.

The schematic diagram of the experimental setup is shown in Fig. 8. In order to obtain a uniform velocity at the entrance of the grooved channel, a bell mouth type of the channel entrance was designed. Pyrex glass and acrylic plate are applied to both sides of the channel and to the bottom of the channel, respectively, for the visualization of the flow inside. The PIV system used in this study consists of a laser, a 480 by 420 resolution CCD camera and a

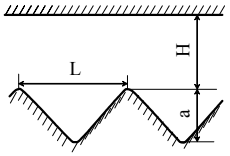

Fig. 7. Grooved channel.

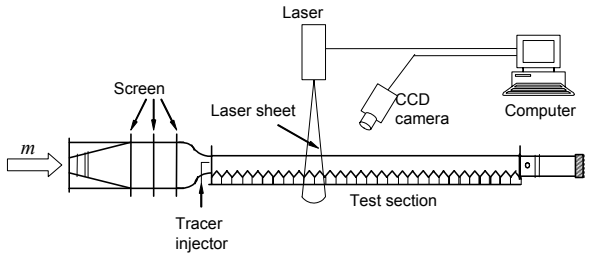

Fig. 8. Schematic diagram of the apparatus.

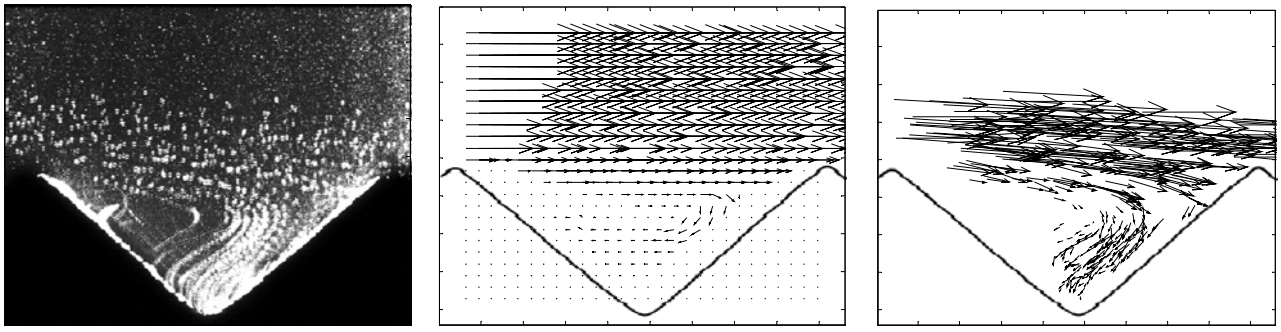

(a) Flow visualization (b) PIV result (c) PTV result.

Fig. 9. Experimental results of simultaneous measurement.

computer which controls the PIV system. The PIV tracer was polystyrene particles having a mean diameter of 25 μm and the PTV particles were also polystyrene particles with diameter range of 200-300 μm. The specific gravity of polystyrene particles is 1.04. The experiment was performed at the condition of steady flow with Re=370.

The larger particles were detected based on the brightness and size of the particles in the CCD image using dynamic threshold-binarization method (Ohmi and Li, 2000). Then an image with the large particles removed leaving only PIV tracer particles was created for PIV analysis to obtain the fluid velocity. Using the locations of the larger particles, the velocity of individual large inertial particles was obtained using PTV.

Figure 9 shows the flow visualization and the results of the simultaneous measurement. The flow visualization was obtained by overlapping 30 successive CCD images taken in the time interval of 3/25 s. There can be found a slow rotating vortex inside the groove and the main stream outside the groove is hardly affected by the recirculating flow within the groove, as shown in the PIV result. Contrary to the fluid, the large particles in the main stream move downward slowly to enter the groove valley. Then the large particles in the groove gradually slow down to deposit onto the groove surface.

The velocities of the large particles in the PTV result are very similar to the behaviors of large particles recognized from the flow visualization result. The fluid velocity measurement is found almost not affected by the existence of the large particles. This indicates the simultaneous measurement method developed in this study is accurate and can be applied to actual cases.

CONCLUSION

A method for simultaneously measuring the fluid velocity and the large particle velocity in a particle-containing fluid flow using a single CCD camera was developed in this study. The fluid velocity and the particle velocity are measured using PIV and PTV, respectively. The images for both the PIV and the PTV analyses are extracted from the native images containing both the small PIV tracer particles and the large particles contained inherently in the fluid. In order to reduce the effect of large particles on the PIV measurement caused by the velocity differences between the fluid and large particles, the mean brightness of small PIV particles is substituted for the locations of large particles in the PIV calculation. The simulation and experimental results showed that the new method can reduce significantly the PIV error caused by the large particles. The new method can be applied to the investigation of particulate fouling problems.

ACKNOWLEDGEMENT

The authors gratefully acknowledge the support of the Carbon Dioxide Reduction and Sequestration R&D Center from the Ministry of Science and Technology, Korea.

NOMENCLATURE

a	groove depth
A	area [pixel^2] or interrogation window
d	displacement [pixel]
E_{mean}	mean value of the PIV evaluation error [-]
f	brightness function of the first interrogation window
g	brightness function of the second interrogation window
H	channel height
l_p	characteristic length of the large [pixel]
L	groove length
n	number of large particles
N	number of interrogation windows

R correlation function
s separation vector [pixel]
X position vector [pixel]
α optimal replacement value for the large particle in the interrogation window f
β optimal replacement value for the large particle in the interrogation window g

Subscripts
f interrogation window A_f
g interrogation window A_g

REFERENCES

Choi, H. M., Kurihara, T., Monji, H. and Matsui, G., 2002, Measurement of particle/bubble motion and turbulence around it by hybrid PIV, *Flow Measurement and Instrumentation*, Vol. 12, 421-428.

Gonzalez, R. C. and Woods, R. E., 2002, Digital Image Processing, 2nd ed., Prentice-Hall, New Jersey.

Jin, D. X., Kim, S. Y., Lee, D. Y., and Lee, Y. P., 2004, PIV investigations of the flow mixing enhancement by pulsatile flow in a crooved channel, *Korean Journal of Air-Conditioning and Refrigeration Engineering*, Vol. 16, 324-331 (in Korean).

Ohmi, K. and Li, H. Y., 2000, Particle-tracking velocimetry with new algorithms, *Measurement Science and Technology*, Vol. 11, 603-616.

Okamoto, K., Nishio, S., Saga, T. and Kobayashi, T., 2000, Standard images for particle-image velocimetry, *Measurement Science and Technology*, Vol. 11, 685-691.

Wereley, S. T., Akonur, A. and Lueptow, R. M., 2002, Particle-fluid velocities and fouling in rotating filtration of a suspension, *Journal of Membrane Science*, Vol. 209, 469-484.

Westerweel, J., 1997, fundamentals of digital particle image velocimetry, *Measurement Science and Technology*, Vol. 8, 1379-1392.